RESULTS

CHAPTER FOUR: RESULTS

4.1 OPTIMIZATION OF MOLECULAR DIAGNOSTIC TECHNIQUES

4.1.1 Polymerase Chain Reaction

Optimization of the PCR was applied to the detection of HHV-6 DNA with first round primers, A and C, and second round primers, HS6AE and HS6AF. Firstly, PCR parameters were modified from Aubin *et al.* (1991) to allow first and second round amplification using one PCR programme.

The primers used in the first round and nested PCR protocol were chosen due to the restriction site that differentiates between HHV-6 variants. Also, these primers were efficient in design as the G + C content was between 54% - 55% and the length of primers, 20-24 bp. Primers were annealed at 60°C which was 5°C below the given melting temperature (T_m) of the nested primers.

In the first cycle, samples were denatured at 92°C for 7 minutes to ensure complete denaturation so that the DNA strands would not reanneal. In the last cycle, the extension step was increased to 7

minutes to ensure complete extension of the target sequences. A total of 40 PCR cycles were performed as the optimum number of cycles required to amplify approximately 1×10^3 target molecules. Too few cycles yielded low target product.

DNA from HHV-6 infected MOLT-3 cells were used as positive control in PCR experiments. The presence of the HHV-6 DNA prior to amplification was verified by immunohistochemistry and *in situ* hybridization. Early PCR assays failed to amplify the 830 bp region of the viral LTP. After careful trouble-shooting, which included varying the concentration of enzyme, primers and Mg ion, it was found that the inclusion of 0.01% (w/v) gelatin in the 10× PCR buffer gave the expected PCR results. Most PCR buffers exclude gelatin as many protocols do not require added protein to help stabilize the enzyme. PCR buffer (10×) containing 0.01% gelatin and 15mM $MgCl_2$ was obtained from Perkin-Elmer Cetus.

Subsequently, optimization of the PCR was performed by varying reagent concentrations in experiments. Results were assayed on agarose gels. The optimal *Taq* DNA polymerase concentration was determined as 2.5U per 50 µl reaction with no change to the magnesium ion concentration. A higher enzyme concentration yielded nonspecific background products which hindered the success of second round PCR.

The addition of 1 µl of dNTP mix into the PCR cocktail supplied 200 µM of each dNTP in equal proportion. A heavy yield was observed in a 2 % agarose gel with no background products.

First and second round amplification was performed using 50 pmol of each primer however the presence of primer-dimers were noted. When the concentration of primers was reduced to 20 pmol, this effect was not seen.

A serial dilution of the positive control revealed the least amount of DNA required for a successful amplification to be between 500 ng and 100 ng. However, upon quantification, it was found that most formalin-fixed, paraffin-embedded tissue contained approximately 100 ng of DNA and the other parameters were optimized around this value.

4.1.2 Nonradioactive *in situ* hybridization

In situ hybridization was optimized to detect HHV-6 DNA sequences with nonradioactive oligonucleotide probes. These variant-specific probes were previously used in DNA dot blot analysis by Dewhurst *et al.* (1993). These probes were labelled by the highly sensitive 3'-tail labelling with Dig-11-dUTP/dATP. This involved independent synthesis of tails varying between 10-100 nucleotides in length. An average tail length of 50 nucleotides incorporates approximately 5 digoxigenin molecules. This

increased the sensitivity of the probes which enabled better detection of the viral DNA (Boehringer Mannheim, 1993).

Since there was no cell line with an established HHV-6 copy number, the sensitivity in terms of copies per cell could not be determined. Nevertheless, HHV-6 infected MOLT-3 cells were used to determine the optimum working concentration of the probe in the hybridization cocktail. This was further readjusted for formalin-fixed, paraffin-embedded tissue.

One of the major problems encountered with *in situ* hybridization was the loss of tissue during the washing procedures after hybridization. To reduce this occurrence, slides were treated with organosilane prior to adhesion of the tissue sections. Organosilane does not wet and so keeps the hybridization buffer in place during hybridization. All incubation and washing steps were performed in the least time possible to avoid unnecessary tissue loss or damage.

Overnight incubation of tissue sections with hybridization buffer had a tendency to dry out. However, proper sealment of the wells containing the tissue sections, with silicone glue eliminated this problem. As an added precaution, the humidified chamber was moistened with 2× SSC to maintain similar vapour pressure with the hybridization buffer.

Permeabilization of cells within tissue sections with Proteinase K improved hybridization signal intensity since it allowed greater

penetration of the probes. Careful optimization by testing a dilution series of the enzyme on infected MOLT-3 cells showed the best concentration to be 50 μg/ml, however this was not the case for paraffin-embedded tissue. The working concentration was finally determined as 100 μg/ml. Incubation time was varied between 15 minutes to 1 hour at 37°C. It was observed that, while incubation for 1 hour greatly improved signal intensity, tissue loss was evident. The incubation time was later reduced to 15 minutes since this step was not a requirement, but merely an addition to obtain intense staining.

Four percent paraformaldehyde was freshly prepared for each batch of slides tested, to prevent the formation of degraded aldehyde byproducts which may increase background staining. Incubation with paraformaldehyde was performed before hybridization to ensure equal fixation. It was found that a 20 minute incubation period at room temperature improved tissue adhesion to the slide. Extended fixation times were not necessary as the tissues had undergone at least 24 of formalin-fixation prior to paraffin-embedding.

4.1.3 Immunohistochemistry

HHV-6 encoded monoclonal antibodies were diluted in a series and each dilution tested with infected MOLT-3 cells. The working concentration was determined by observation of optimum specific staining with minimal background (maximum signal to noise ratio). The antibody incubation time was preset to 1 hour at room temperature. Incubation at higher temperatures to reduce the incubation time yielded increased nonspecific background staining and so was not feasible.

The use of the LSAB Kit and the AEC substrate Kit did not require optimization and was used directly in the protocol.

4.2 ANALYSIS OF PARAFFIN-EMBEDDED TISSUE BIOPSIES OF THE ORAL MUCOSA

Sixty five formalin-fixed and paraffin-embedded oral tissue of various histopathological status were pooled for this study, of which 22 cases were obtained from the Seremban General Hospital and 43 cases from the Dental Faculty of Universiti Malaya. These cases were biopsied from the buccal sulcus, palate, tongue, floor of mouth and gingiva of patients. All cases were subjected to H and E examination and the histology diagnosed by pathologists based on the definition as recommended by WHO (Sobin *et al.*, 1978).

The oral tissue cases were classified into histopathological groups, namely malignant tumours, premalignant lesions and normal tissue of unremarkable pathology (Table 4.1). Table 4.2 further distributes the cases by race and gender of individuals from which oral biopsies were obtained.

Table 4.1: Histology of paraffin-embedded tissue biopsies of the oral mucosa

Histological Type	No. of cases
Malignant	**42**
Keratinizing squamous cell carcinoma	29
Nonkeratinizing squamous cell carcinoma	13
Premalignant	**13**
Leukoplakia	6
Lichen planus	7
Normal	**10**
Total	**65**

Table 4.2: Distribution of individuals from which oral biopsies were obtained by race and sex

	Malignant		Premalignant		Normal	
Race	**M**	**F**	**M**	**F**	**M**	**F**
Malay	2	2	1	2	2	1
Indian	8	21	0	5	1	4
Chinese	7	2	3	2	2	0
Total	17	25	4	9	5	5

M : Male

F : Female

4.2.1 Amplification of HHV-6 DNA sequences in oral tissue and analysis of PCR products

DNA extracted from 65 formalin-fixed, paraffin-embedded oral tissue sections was subjected to PCR amplification for the β-globin gene sequence to establish the quality of DNA. Only those samples that amplified a 268 bp fragment of the β-globin gene were included in the study.

The presence of HHV-6 DNA sequences in oral tissues was detected by nested PCR. All PCR experiments were run concurrently with positive and negative controls and results were as expected. First round PCR with external primers A and C amplified a 830 bp fragment of the HHV-6 LTP gene. None of the cases showed any amplification in the first round. Second round PCR with internal primers, HS6AE and HS6AF amplified an approximately 750 bp fragment within the 830 bp fragment (Fig. 4.1). Of the 42 oral SCC cases studied, 11 (26.2%) were HHV-6 positive.

Southern hybridization of nested PCR products with labelled pZVH14 was carried out to confirm the specificity of PCR amplification (Fig. 4.2). HHV-6 was detected in an additional 6 oral SCC cases, previously undetected on agarose gel electrophoresis, bringing the total to 17/42 (40.5%) HHV-6 positive SCC cases. Normal oral tissue examined for

HHV-6 DNA were negative by nested PCR and hybridization. Table 4.3 summarizes the results of nested PCR and Southern hybridization of HHV-6 DNA sequences.

HHV-6 was present in more SCC cases compared to the other oral lesions, especially in keratinizing SCC cases in which 27.6% positivity was detected by nested PCR and 44.8% by Southern hybridization. The presence of HHV-6 DNA in premalignant leukoplakic lesions was observed in 2 (33.3%) cases by Southern hybridization while 1 (14.3%) lichen planus lesion was positive for HHV-6 DNA sequences.

Restriction endonuclease digestion was carried out on nested PCR products which amplified HHV-6 DNA sequences of approximately 750 bp in size. HHV-6 B variants contain an internal restriction site for *Hin*d III within the LTP gene sequence of 750 bp. Variant A strains lack this restriction site, therefore allowing differentiation between the variants.

A total of 13 oral samples were subjected to digestion by *Hin*d III and resolved on a 2% agarose gel (Fig. 4.3). HHV-6 variant B sequences were cleaved into 2 fragments of approximately 220 and 530 basepairs. Six of eleven (54.5%) SCC cases positive for HHV-6, were of type A and 5/11 (45.5%), type B (Table 4.4). In the keratinizing SCC cases, it was interesting to note that variants A and B were present in equal proportion.

Table 4.3: Prevalence of HHV-6 DNA in paraffin-embedded oral tissue detected by PCR and Southern hybridization.

Histological Type	Total samples	HHV-6 positive (%)	
		Nested PCR	Southern hybridization
Keratinizing squamous cell carcinoma	29	8 (27.6)	13 (44.8)
Nonkeratinizing squamous cell carcinoma	13	3 (23.1)	4 (30.8)
Leukoplakia	6	1 (16.7)	2 (33.3)
Lichen planus	7	1 (14.3)	1 (14.3)
Normal	10	0	0

Table 4.4: Variant classification of HHV-6 positive oral tissue by restriction enzyme analysis

Histology	HHV-6 variant A (750 bp)	HHV-6 variant B (220 bp, 530 bp)	Total positive
Keratinizing SCC	4	4	8/29
Nonkeratinizing SCC	2	1	3/13
Leukoplakia	1	0	1/6
Lichen planus	0	1	1/7

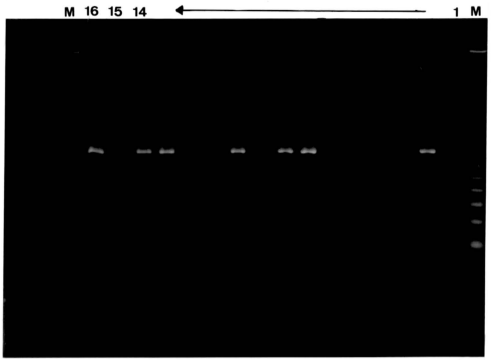

Figure 4.1: Nested PCR amplification of HHV-6 DNA sequences from paraffin-embedded oral lesions visualized on ethidium bromide-stained agarose gel.

Lane M : 100 bp molecular weight marker

Lane 1-14 : DNA from oral SCC patients

Lane 15 : HHV-6 negative control (water)

Lane 16 : HHV-6 positive control

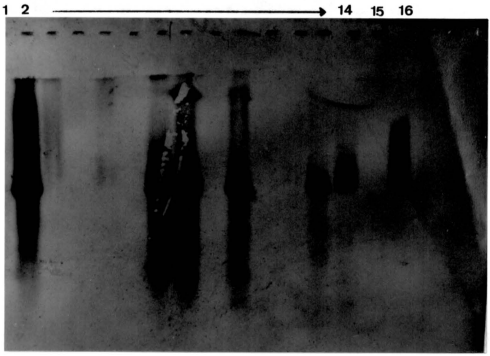

Figure 4.2: Southern blot hybridization of PCR amplified HHV-6 DNA sequences from paraffin-embedded oral lesions.

Lane 1-14 : DNA from oral SCC patients

Lane 15 : HHV-6 negative control (water)

Lane 16 : HHV-6 positive control

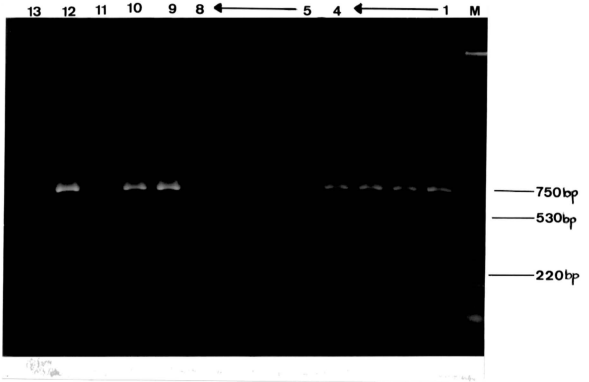

Figure 4.3: Restriction digestion pattern of the PCR-amplified 750 bp fragment visualized by ethidium bromide-stained agarose gel

Lane M : 100 bp molecular weight marker

Lane 1-4, 9, 10 : Uncleaved sample DNA fragment indicative of HHV-6 A type DNA

Lane 5-8, 11 : Cleaved DNA fragment indicative of HHV-6 B type DNA

Lane 12 : Undigested HHV-6 positive control (strain Z29)

Lane 13 : Digested HHV-6 positive control (strain Z29)

4.2.2 Nonradioactive detection of HHV-6 DNA in oral tissue

HHV-6 probe A and B reacted with acetone-fixed HHV-6 infected MOLT-3 cells. Intense hybridization signal was observed in the nuclei of infected cells (Fig. 4.4). Uninfected MOLT-3 cells showed no reaction with the probes (Fig. 4.5). NISH not only detected the presence of HHV-6 DNA sequences in epithelial cell nuclei of the oral mucosa but distinguished the variants present within the same sample. Table 4.5 summarizes the results. It was noted the *in situ* hybridization increased the sensitivity of HHV-6 detection. The use of 3'-tail labelled probes facilitated the detection of HHV-6 fragments within the nucleus of infected cells.

A total of 33/42 (78.6%) oral SCC cases showed the presence of HHV-6 DNA sequences in which 16 (38.1%) cases hybridized with both HHV-6 variant A and B probes. HHV-6 variant A sequences alone were found in 3 (7.1%) cases whereas HHV-6 B alone was found in 14 (33.3%) cases. The presence of HHV-6 by NISH was observed in the nuclei of tumour cells, the target region and occasionally in normal columnar epithelial cells in the oral mucosa.

The distribution of hybridization signals in oral SCC tissue sections was described as being either uniform, patchy or scattered. Signal distribution was described as uniform when most of the cells in the target

region were positive, patchy when staining was in several areas only and scattered when very few cells stained positive.

Most of the SCC cases that stained positive for HHV-6 A or B were found in the tumour region, however the signal distribution was either uniform (Fig. 4.6) or patchy. Two cases were stained positive for HHV-6 DNA only in the nuclei of normal columnar epithelial cells lining the duct-like structures within the oral mucosa. HHV-6A DNA sequences were also observed in both the tumour and normal cells of 3 cases, in which the distribution was patchy.

Four cases contained HHV-6B DNA sequences distributed uniformly in both the tumour and the columnar epithelial cell nuclei. In the keratinizing SCC cases, a common histologic feature is the presence of keratin/epithelial pearls. In some of these cases, HHV-6 DNA sequences were demonstrable in the cells surrounding the keratin pearls (Fig. 4.7). HHV-6 positivity exceeded 75% in both types of SCC, with more nonkeratinizing cases staining positive for HHV-6 DNA sequences than keratinizing SCC. Based on this study, HHV-6 variant B DNA sequences were predominant over the A variant in both keratinizing and nonkeratinizing SCC tissues.

It was interesting to note that all 6 premalignant leukoplakia cases studied showed the presence of HHV-6 DNA sequences. Also 6

(85.7%) of the 7 lichen planus lesions hybridized to the HHV-6 probes. The distribution of these signals was mostly uniform in the site of leukoplakic and lichen planus lesions. HHV-6 DNA sequences were also found in 5/10 (50%) normal cases in which a uniform distribution of positively stained epithelial cells was observed in the oral mucosa (Fig. 4.8).

Table 4.5: Prevalence of HHV-6 DNA detected by *in situ* hybridization with variant-specific oligonucleotides in oral tissue.

Histological Type	Total samples	HHV-6 A (%)	HHV-6 B (%)	HHV-6 A and B (%)	Total positive
Keratinizing squamous cell carcinoma	29	2 (6.9)	10 (34.5)	10 (34.5)	22 (75.9%)
Nonkeratinizing squamous cell carcinoma	13	1 (7.7)	4 (30.8)	6 (46.1)	11 (84.6%)
Leukoplakia	6	2 (33.3)	0	4 (66.7)	6 (100%)
Lichen planus	7	1 (14.3)	1 (14.3)	4 (57.1)	6 (85.7%)
Normal	10	2 (20.0)	0	3 (30.0)	5 (50.0%)

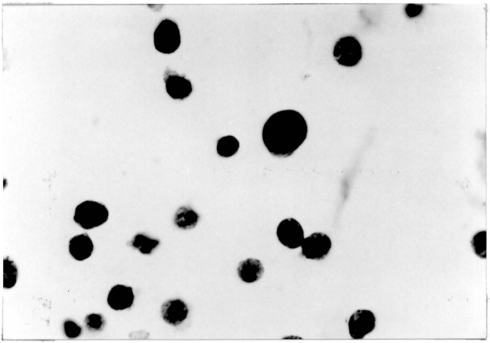

Figure 4.4: Intense *in situ* hybridization signal in the nuclei of HHV-6-infected MOLT-3 cells (400×).

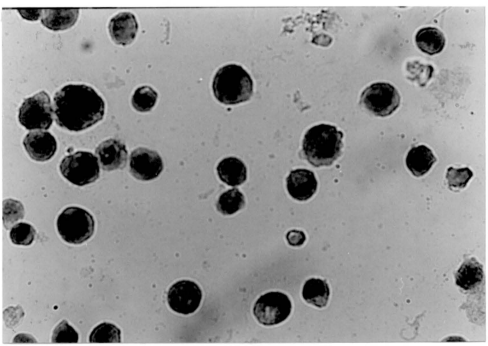

Figure 4.5: Control reaction in which no hybridization signal was observed with uninfected MOLT-3 cells (400×).

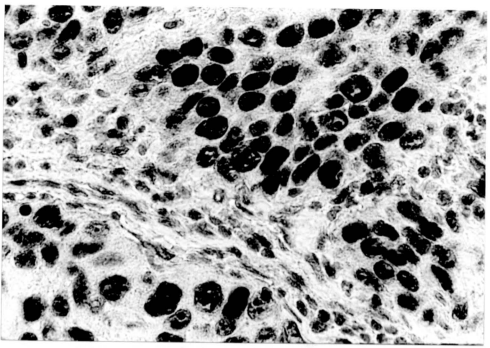

Figure 4.6: NISH signal (dark purple) for HHV-6A localized in the nuclei of a well differentiated keratinizing squamous cell carcinoma of the oral mucosa (400×).

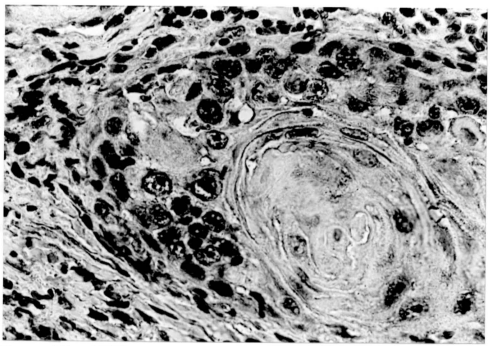

Figure 4.7: NISH positive staining for HHV-6B in the outer layer of cells (dark purple) surrounding a keratin pearl from a well differentiated keratinizing SCC of the oral mucosa (400×).

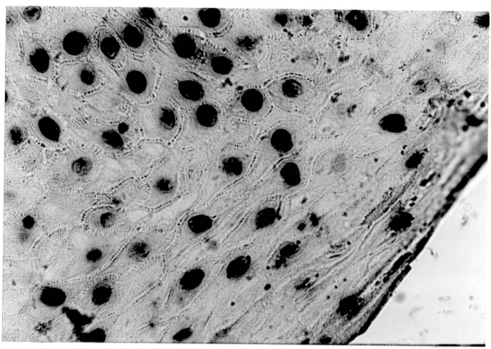

Figure 4.8: NISH signal for HHV-6B in the nuclei of squamo-epithelial cells of a normal oral tissue sample (400×).

4.2.3 Expression of HHV-6 encoded proteins in oral tissue

Monoclonal antibodies against HHV-6 p41/38 early antigen and HHV-6 gp116/64/54 late antigen localized these proteins in the nuclei or cytoplasm of HHV-6 infected MOLT-3 cells. Intense nuclear and/or cytoplasmic staining was observed in these cells (Fig. 4.9). Uninfected MOLT-3 cells illicited no response with the MAbs (Fig. 4.10). Expression of HHV-6 encoded p41/38 and gp116/64/54 was observed in the nuclei and/or cytoplasm of oral tissue studied.

Table 4.6 shows the prevalence of the two viral antigens investigated and Table 4.7 shows the immunolocalization of HHV-6 positive signals within the cells. Intense nuclear or cytoplasmic staining was observed in the target region, that is, the tumour cells (Fig. 4.11) and sometimes also in the columnar epithelial cells lining ductal walls.

A total of 37/42 (88.1%) oral SCC cases showed the presence of HHV-6 antigens in which the majority of cases localized the viral antigens in both the cytoplasm and nuclei of tumour cells. Two SCC cases expressed gp116/64/54 and one case expressed p41/38 in columnar epithelial cells only while the tumour regions were negatively stained. However, 3 SCC cases expressed gp116/64/54 in both the tumour and columnar epithelial cells, uniformly distributed. HHV-6 gp116/64/54 was

localized in 19/42 (45.2%) SCC cases and the expression of p41/38 was observed in 4/42 (9.5%) cases. The late antigen gp116/64/54 was also found concurrently with p41/38 early antigen in 14/42 (33.3%) cases. Viral proteins were expressed in all nonkeratinizing SCC tissue and lichen planus lesions.

It was interesting to note that keratin pearls in the invasive keratinizing SCC cases also stained positive for viral protein expression (Fig. 4.12) that is, 5/29 (17.2%) cases for p41/38 and 10/29 (34.5%) cases for gp116/64/54. To eliminate the possibility of non-specific staining in the keratin pearls, cytokeratin (Biogenex Lab.) was allowed to adsorb to the MAbs prior to viral antigen studies. Positive staining was still observed in the keratin pearls.

In addition, some keratinizing SCC cases did not stain for viral antigen expression in the keratin pearls showing that positive staining in the other keratin pearls were specific. HHV-6 DNA sequences were also detected in an outer layer of cells surrounding these epithelial pearls by NISH suggesting that viral proteins expressed by HHV-6 infected cells surrounding the keratin pearls get trapped by the keratin and remain there.

Immunohistochemical staining in leukoplakic and lichen planus lesions was either patchy or uniform, distributed mainly in the cell

nuclei and in half the cases, the cytoplasm also. Five (50%) out of 10 normal oral tissue localized HHV-6 proteins in the cytoplasm and nuclei of epithelial cells lining ducts.

Table 4.6: Immunolocalization of HHV-6 specific antigens in the cytoplasm and/or nucleus of paraffin-embedded oral tissue

Histological Type	Total samples	Reactivity to virus-encoded antigens (%)			Total positive
		p41/38	gp116/64/54	p41/38 and gp116/64/54	
Keratinizing squamous cell carcinoma	29	3 (10.3)	10 (34.5)	11 (37.9)	24 (82.8%)
Nonkeratinizing squamous cell carcinoma	13	1 (7.7)	9 (69.2)	3 (23.1)	13 (100%)
Leukoplakia	6	0	3 (50.0)	1 (16.7)	4 (66.7%)
Lichen planus	7	0	5 (71.4)	2 (28.6)	7 (100%)
Normal	10	0	2 (20.0)	3 (30.0)	5 (50.0%)

Table 4.7: Immunolocalization of HHV-6 p41/38 and gp116/64/54 in paraffin-embedded oral tissue

Histological Type	Total positive	Cytoplasm	Nucleus	Cytoplasm and Nucleus
Squamous cell carcinoma	37	12 (32.4)	2 (5.4)	23 (62.2)
Leukoplakia	4	0	2 (50.0)	2 (50.0)
Lichen planus	7	0	4 (57.1)	3 (42.9)
Normal	5	0	0	5 (100)

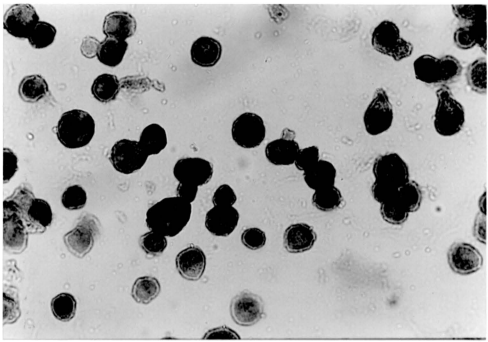

Figure 4. 9: Intense cytoplasmic staining (reddish brown) for gp116/64/54 in HHV-6-infected MOLT-3 cells (400×).

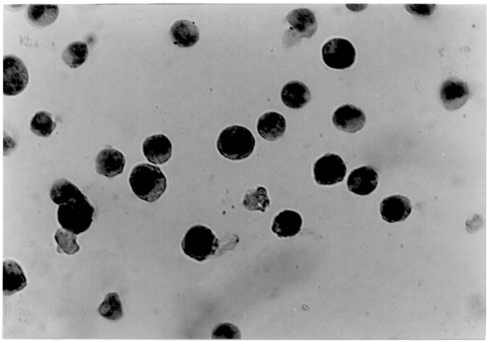

Figure 4.10: Control reaction in which no staining was observed with uninfected MOLT-3 cells, counterstain with Mayer's hematoxylin shows the nuclei stained blue (400×).

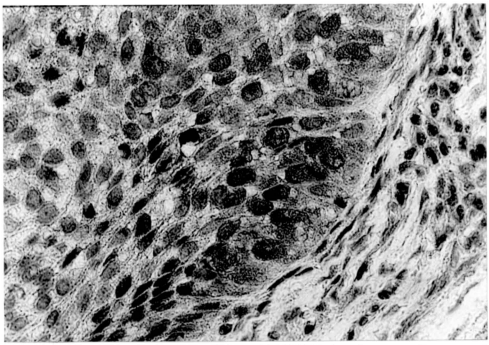

Figure 4.11: IHC positive for HHV-6 gp116/64/54 in the cytoplasm and nuclei of a well differentiated keratinizing SCC of the oral mucosa (400×).

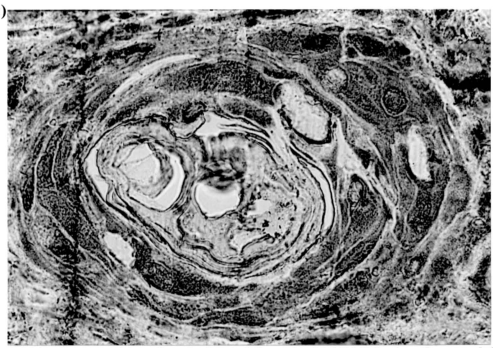

Figure 4.12: Immunohistochemical staining (gp116/64/54) in the nuclei and cytoplasm of cells in a keratin pearl and its' outer layer (400×).

4.3 ANALYSIS OF FORMALIN-FIXED, PARAFFIN-EMBEDDED TISSUE BIOPSIES OF THE SALIVARY GLANDS

A total of 18 tissue biopsies from the parotid gland and the submandibular gland were obtained from Seremban General Hospital. Table 4.8 shows the histopathology of these samples. These biopsies were taken from individuals between the ages 1 and 70 of the 3 major ethnic groups, Malay, Indian and Chinese.

Table 4.8: Histology of paraffin-embedded salivary gland tissue biopsies of the salivary gland

Histological Type	No. of cases
Malignant	**7**
Squamous cell carcinoma	3
Mucoepidermoid carcinoma	4
Benign	**6**
Pleomorphic adenoma	5
Adenolymphoma	1
Normal	**5**
Total	**18**

4.3.1 Amplification of HHV-6 DNA sequences in salivary gland tissue and analysis of PCR products

Eighteen formalin-fixed, paraffin-embedded tissue biopsies of the salivary glands were subjected to amplification of the β-globin gene sequence to verify the presence of PCR-viable DNA. All cases studied amplified a 268 bp fragment of the β-globin gene.

Following this, 10 µl of each sample was used as template in the first round PCR. One microlitre of the amplified product was reamplified using the nested protocol. First round PCR did not amplify any HHV-6 DNA sequences, nested PCR amplified HHV-6 DNA in only 1 (33.3%) SCC tissue (Fig. 4.13). Southern hybridization of PCR products with labelled pZVH14 (Fig. 4.14) revealed 2 more HHV-6 positive samples (Table 4.9).

Two out of 5 (40%) normal salivary gland tissue showed the presence of HHV-6 following Southern hybridization. With the exception of 1/3 (33.3%) of the SCC cases being positive for HHV-6 by PCR, all the rest were negative. Restriction enzyme analysis of the HHV-6 positive SCC case revealed the variant to be of type A.

Table 4.9: Prevalence of HHV-6 DNA in paraffin-embedded salivary gland tissue detected by PCR and Southern hybridization

Histological Type	Total samples	HHV-6 positive (%)	
		Nested PCR	Southern hybridization
Squamous cell carcinoma	3	1 (33.3)	1 (33.3)
Mucoepidermoid carcinoma	4	0	0
Pleomorphic adenoma	5	0	0
Adenolymphoma	1	0	0
Normal	5	0	2 (40)

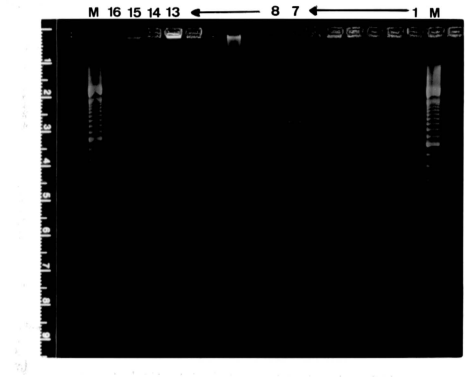

Figure 4.13: Nested PCR amplification of HHV-6 DNA sequences from paraffin-embedded salivary gland tissue visualized on ethidium bromide-stained agarose gel.

Lane M : 100 bp molecular weight marker

Lane 1-7 : DNA from salivary gland carcinoma biopsies

Lane 8-13 : DNA from benign salivary gland tumour biopsies

Lane 14 : HHV-6 negative control (empty paraffin wax block)

Lane 15 : HHV-6 positive control

Lane 16 : HHV-6 negative control (water)

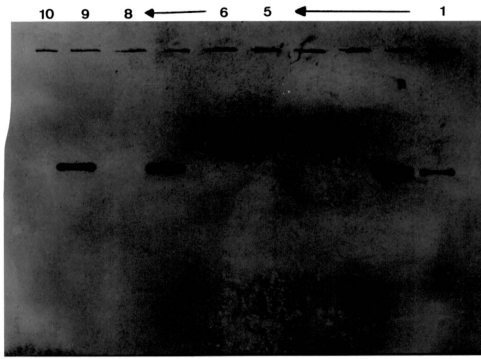

Figure 4.14: Southern blot hybridization of PCR amplified HHV-6 DNA sequences from paraffin-embedded salivary gland tissue.

Lane 1-5 : DNA from normal salivary gland biopsies

Lane 6-8 : DNA from salivary gland carcinoma (SCC) biopsies

Lane 9 : HHV-6 positive control

Lane 10 : HHV-6 negative control (water)

4.3.2 Nonradioactive detection of HHV-6 DNA sequences in salivary gland tissue

Reaction was observed as a purple staining in the nuclei of target cells within the salivary gland tissue. The target cells were the tumour region in both the malignant and benign tumours whereas in the controls, the target cells were the epithelial cells of the oral mucosa. Table 4.10 shows the presence of HHV-6 variant A and B in the salivary gland tissue sections of various pathology.

Of the 7 malignant carcinoma, 6 (85.7%) showed the presence of HHV-6 DNA sequences (Fig. 4.15) in which variant B was predominant over variant A. It was found that the one SCC case positive for HHV-6 A by PCR hybridized to both HHV-6 A and B probes. The distribution of hybridization signals in these tissues was patchy. All 5 of the benign pleomorphic adenoma tumours localized HHV-6 variant A and B DNA sequences. The distribution was mostly uniform. The benign lymphoadenoma did not hybridize to either probe.

Three (60%) of the normal salivary gland tissue hybridized with the HHV-6 B probe alone. The signal was localized in columnar epithelial cells lining ducts (Fig. 4.16), serous and mucous acinic cells. The distribution in each positive tissue sample was uniform. Figure 4.17 shows a normal tissue sample negatively stained for HHV-6.

Table 4.10: Prevalence of HHV-6 DNA detected by *in situ* hybridization with variant specific oligonucleotides in salivary gland tissue

Histological Type	Total samples	HHV-6 A (%)	HHV-6 B (%)	HHV-6 A and B (%)	Total positive
Squamous cell carcinoma	3	0	1 (33.3)	2 (66.7)	3 (100%)
Mucoepidermoid carcinoma	4	0	2 (50.0)	1 (25.0)	3 (75.0%)
Pleomorphic adenoma	5	1 (20.0)	2 (40.0)	2 (40.0)	5 (100%)
Adenolymphoma	1	0	0	0	0
Normal	5	0	3 (60.0)	0	3 (60.0%)

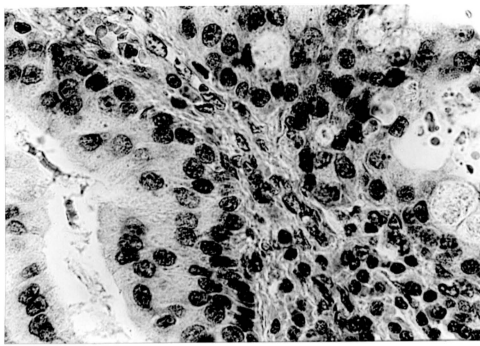

Figure 4.15: NISH signal (dark purple) for HHV-6A in the nuclei of a mucoepidermoid carcinoma of the salivary gland (400×).

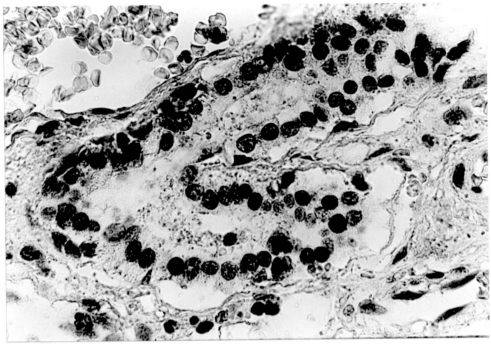

Figure 4.16: NISH positive for HHV-6B in the nuclei of cells lining a duct from a normal salivary gland tissue (400×).

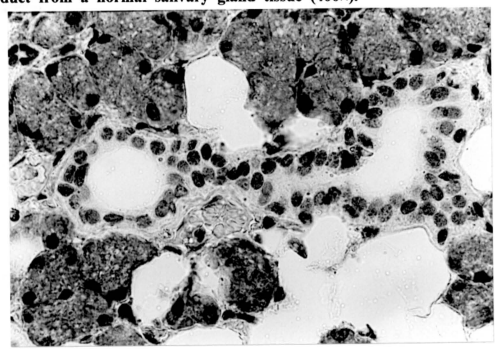

Figure 4.17: Normal salivary gland tissue showing a duct negatively stained for HHV-6. The nucleus has been counterstained with Mayer's hematoxylin (400×).

4.3.3 Expression of HHV-6 encoded proteins in salivary gland tissue

The salivary gland tissue sections were examined concurrently with the appropriate positive and negative controls. Nuclear and cytoplasmic staining was observed in the various tumours and normal tissue with both MAbs that react to gp116/64/54 and p41/38. Table 4.11 summarizes the results.

It is very interesting to note that every single tissue studied expressed HHV-6 antigens and the presence of p41/38 was always accompanied by the expression of gp116/64/54. It was clearly seen that gp116/64/54 was found in abundance in these tissues. Expression of viral proteins correlated with the localization of HHV-6 DNA sequences by NISH. Only 2 cases did not correspond with antigen expression. The expression of gp116/64/54 in each SCC tissue was distributed evenly in the tumour regions (Fig. 4.18) however, the expression of p41/38 in the one case was patchy. Each mucoepidermoid carcinoma case studied expressed gp116/64/54 distributed evenly in the tumour cells and cells lining ducts. Expression of p41/38 was distributed in certain areas of the cytoplasm of tumour cells.

Expression of gp116/64/54 was observed in the nuclei and/or cytoplasm of all 5 pleomorphic adenoma cases studied. Staining was

distributed in the tumour region and also in the cells lining well formed ducts. The one adenolymphoma case studied also expressed gp116/64/54 in the target region, composed of columnar or cubical epithelial cells that formed columns, which was a common feature of this tumour.

Four cases of normal pathology studied as controls expressed only gp116/64/54 in the cytoplasm of columnar epithelial cells lining ducts (Fig. 4.19) and lumen. Staining was distributed evenly in 3 cases while in one case, only a few ductal cells were positive. One normal case expressed both gp116/64/54 and p41/38 in the nucleus and cytoplasm of columnar epithelial, serous and mucous cells of the tissue. Staining was distributed evenly.

Table 4.11: Prevalence of HHV-6 encoded proteins in paraffin-embedded salivary gland tissue

Histological Type	Total samples	Reactivity to virus-encoded antigens (%)			Total positive
		p41/38	gp116/64/54	p41/38 and gp116/64/54	
Squamous cell carcinoma	3	0	2 (66.7)	1 (33.3)	3
Mucoepidermoid carcinoma	4	0	2 (50.0)	2 (50.0)	4
Pleomorphic adenoma	5	0	5 (100)	0	5
Adenolymphoma	1	0	1 (100)	0	1
Normal	5	0	4 (80.0)	1 (20.0)	5

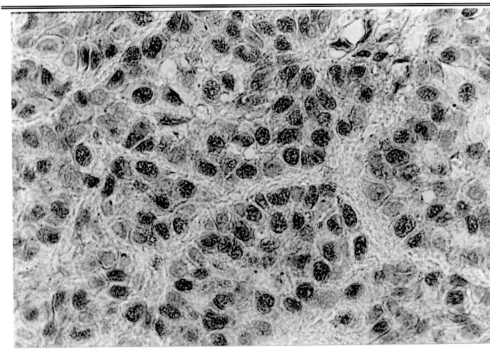

Figure 4.18: Immunohistochemical staining (reddish brown) of HHV-6 gp116/64/54 in the nuclei of a squamous cell carcinoma of the salivary gland (400×).

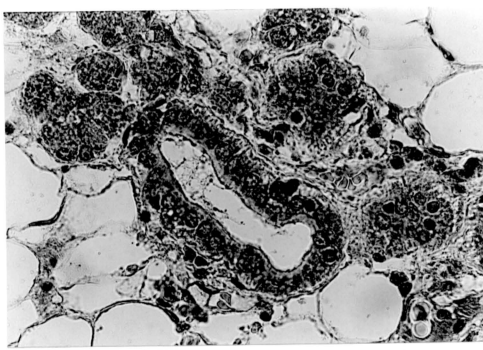

Figure 4.19: Immunohistochemical staining of HHV-6 gp116/64/54 in the cytoplasm of columnar epithelial cells lining a duct from a normal salivary gland tissue (400×).

4.4 ANALYSIS OF PARAFFIN-EMBEDDED TISSUE BIOPSIES OF THE CERVICAL MUCOSA

Thirty-eight formalin-fixed and paraffin-embedded cervical tissue biopsies were available for this study of which 30 were carcinoma cases and 8 were normal. Table 4.12 classifies the tissue by histology based on H and E examination by pathologists. The racial distribution of individuals from whom these biopsies were obtained is tabulated in Table 4.13.

Table 4.12: Histology of paraffin-embedded tissue biopsies of the cervical mucosa

Histological Type	No. of cases
Malignant	**30**
Keratinizing squamous cell carcinoma	11
Nonkeratinizing squamous cell carcinoma	12
Adenocarcinoma	3
Carcinoma *in situ*	4
Normal	**8**
Total	**38**

Table 4.13: Racial distribution of individuals from whom cervical biopsies were obtained

Histological Type	Total samples	Malay	Indian	Chinese
Keratinizing squamous cell carcinoma	9	5	3	1
Nonkeratinizing squamous cell carcinoma	12	3	2	7
Adenocarcinoma	3	1	0	2
Carcinoma *in situ*	4	0	1	3
Normal	8	3	3	2

4.4.1 Amplification of HHV-6 DNA sequences in cervical tissue and analysis of PCR products

PCR amplification was performed with appropriate positive and negative controls, including β-globin gene sequence amplification and the results were as expected. Nested PCR followed by Southern hybridization, confirmed PCR specificity as is shown in Table 4.14. First round PCR did not reveal any positive cases, and so is not tabulated.

Of the 30 cases histologically diagnosed as cervical carcinoma, 10 (33.3%) were positive for HHV-6 as determined by nested PCR amplification (Fig. 4.20) and Southern hybridization (Fig. 4.21). Of these, carcinoma *in situ* (CIS) cases reported the highest percentage of HHV-6 infection. Among the SCC tissue, a higher prevalence of HHV-6 was noted in the nonkeratinizing SCC type. Only one (12.5%) of the 8 normal tissue studied as controls amplified a 750 bp fragment of HHV-6 DNA.

Restriction enzyme analysis of the HHV-6 positive cervical carcinoma showed that 9/10 (90%) were of variant B (Table 4.15). HHV-6 variant A was found in only 1 CIS case.

Table 4.14: Prevalence of HHV-6 DNA in paraffin-embedded cervical tissue detected by PCR and Southern hybridization

Histological Type	Total samples	HHV-6 positive (%)	
		Nested PCR	Southern hybridization
Keratinizing squamous cell carcinoma	11	1 (9.1)	1 (9.1)
Nonkeratinizing squamous cell carcinoma	12	4 (33.3)	4 (33.3)
Adenocarcinoma	3	2 (66.7)	2 (66.7)
Carcinoma *in situ*	4	3 (75)	3 (75)
Normal	8	1 (12.5)	1 (12.5)

Table 4.15: Variant classification of HHV-6 positive cervical tissue by restriction enzyme analysis

Histological Type	HHV-6 variant A (750 bp)	HHV-6 variant B (220 bp, 530 bp)	Total positive
Keratinizing squamous cell carcinoma	0	1	1/11
Nonkeratinizing squamous cell carcinoma	0	4	4/12
Adenocarcinoma	0	2	2/3
Carcinoma *in situ*	1	2	3/4
Normal	0	1	1/8

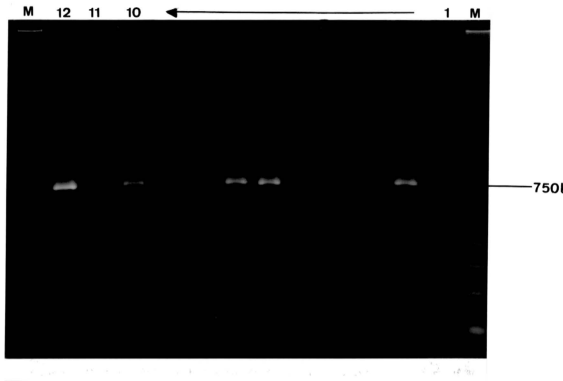

Figure 4.20: Nested PCR amplification of HHV-6 DNA sequences from paraffin-embedded cervical lesions visualized on ethidium bromide-stained agarose gel.

Lane M : 100 bp molecular weight marker

Lane 1-10 : DNA from cervical SCC biopsies

Lane 11 : HHV-6 negative control (water)

Lane 12 : HHV-6 positive control

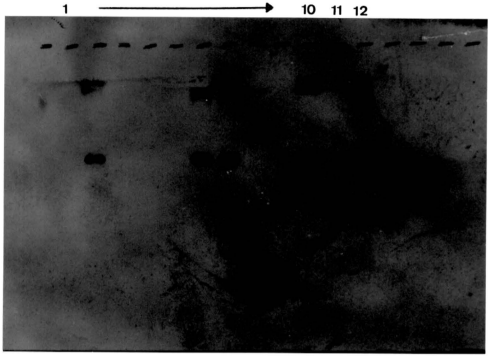

Figure 4.21: Southern blot hybridization of PCR amplified HHV-6 DNA sequences from paraffin-embedded cervical lesions.

Lane 1-10 : DNA from cervical SCC biopsies

Lane 11 : HHV-6 negative control

Lane 12 : HHV-6 positive control

4.4.2 Nonradioactive detection of HHV-6 DNA sequences in cervical tissue

Tissue sections of the 38 cervical tissue were analysed for HHV-6 DNA sequences by NISH using variant specific oligonucleotide probes. Hybridization signals were observed in the nuclei of tumour cells (target region) (Fig. 4.22). Table 4.16 summarizes the results.

Out of the 30 cervical carcinoma cases, 5 (16.7%) showed positive staining for HHV-6 variant B and only 2 cases (6.7%) were positive for HHV-6 variant A DNA. Three (10%) cases reacted with both probe A and B showing the presence of two variants within the same tissue section. HHV-6 variant B was predominantly found in HHV-6 infection.

Mixed infection was observed in 2/11 (18.2%) keratinizing SCC cases localized in the nuclei of tumour cells in a uniform distribution. One of these cases also localized viral DNA in the cells surrounding the invasive tumour (non-tumour region). Chen *et al.* (1994b) observed nucleolar sparing within the cervical tissue they studied, this feature was also noted in the tissue section.

One (25%) out of 4 CIS cases localized HHV-6 A and B in the columnar epithelial cells lining glandular ducts and in the target region.

HHV-6 DNA sequences were also localized in the koilocytes (vacuolated cells) of a CIS case, in this instance, infection was of variant B type (Fig. 4.23).

Two out of 3 ADC cases had HHV-6 DNA sequences distributed evenly in the tumour and surrounding cells. Of the 8 normal cervical tissue studied, 1 (12.5%) sample reacted with HHV-6 probe B and hybridization signal was observed in the nuclei of columnar epithelial cells lining various ducts. This corresponded with PCR studies in which restriction analysis confirmed the HHV-6 infection to be of type B.

Table 4.16: The prevalence of HHV-6 DNA detected by *in situ* hybridization with variant-specific oligonucleotides in cervical tissue

Histological Type	Total samples	HHV-6 A (%)	HHV-6 B (%)	HHV-6 A and B (%)	Total positive (%)
Keratinizing squamous cell carcinoma	11	0	1 (9.1)	2 (18.2)	3 (27.3)
Nonkeratinizing squamous cell carcinoma	12	1 (8.3)	2 (16.7)	0	3 (25.0)
Adenocarcinoma	3	1 (33.3)	1 (33.3)	0	2 (66.7)
Carcinoma *in situ*	4	0	1 (25.0)	1 (25.0)	2 (50.0)
Normal	8	0	1 (12.5)	0	1 (12.5)

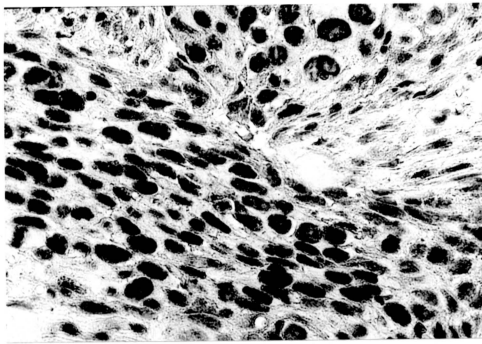

Figure 4.22: NISH signal (dark purple) for HHV-6B localized in the nuclei of an invasive keratinizing squamous cell carcinoma of the cervix (400×).

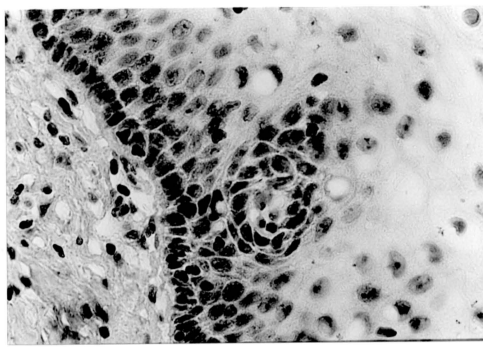

Figure 4.23: NISH signal for HHV-6B in the nuclei of a carcinoma *in situ* of the cervix, hybridization signal was also noted in koilocytes (400×).

4.4.3 Expression of HHV-6 encoded proteins in cervical tissue

Table 4.17 shows the distribution of HHV-6 antigen expression in the various tissues studied. A total of 14/30 (46.7%) diseased tissues and 5/8 (62.5%) normal tissue were positive for HHV-6 encoded proteins. Intense nuclear or cytoplasmic staining, sometimes both, was observed in the tumour cells of cervical carcinomas (target region) (Table 4.18). HHV-6 gp116/64/54 was localized in 6/30 (20%) carcinoma cases while expression of p41/38 early antigen was observed in 3/30 (10%) cases. Both p41/38 and gp116/64/54 were found concurrently in 5/30 (16.7%) cervical carcinoma cases (Fig. 4.24).

Three out of 4 CIS cases stained positive for HHV-6 proteins in the nuclei of both tumour cells and columnar epithelial cells lining ductal walls. All 3 ADC cases studied stained positive for HHV-6 antigens in the target region.

Expression of gp116/64/54 in the nonkeratinizing SCC cases was localized in the target nuclei and cytoplasm of 2 cases. The presence of both p41/38 and gp116/64/54 was observed in the nuclei of tumour cells. Of the 4 keratinizing SCC cases positive for HHV-6 antigens, p41/38 expression in 2 cases was observed in the nuclei of tumour cells and gp116/64/54 expression was localized in the cytoplasm of 1 case. Overall,

HHV-6 gp116/64/54 was observed in more cases compared to p41/38 in all the cervical tissue studied.

Of the 8 normal cervical tissue studied, 3 (37.5%) expressed gp116/64/54 and 1 (12.5%) expressed p41/38 in the cytoplasm of epithelial cells. The expression of both viral antigens was observed in the cytoplasm and nuclei of 1 normal case which corresponded with HHV-6 DNA studies by NISH and PCR. Expression was observed in the endocervical ciliated columnar epithelial cells and some cells in the subepithelial mucosa of the cervix uteri (Fig. 4.25).

Table 4.17: Prevalence of HHV-6 specific antigens in the cytoplasm and/or nucleus of paraffin-embedded cervical tissue

Histological Type	Total samples	Reactivity to virus-encoded antigens (%)			Total positive
		p41/38	gp116/64/54	p41/38 and gp116/64/54	
Keratinizing squamous cell carcinoma	11	2 (18.2)	1 (9.1)	1 (9.1)	4 (36.4%)
Nonkeratinizing squamous cell carcinoma	12	0	2 (16.7)	2 (16.7)	4 (33.3%)
Adenocarcinoma	3	0	1 (33.3)	2 (66.7)	3 (100%)
Carcinoma *in situ*	4	1 (25.0)	2 (50.0)	0	3 (75.0%)
Normal	8	1 (12.5)	3 (37.5)	1 (12.5)	5 (62.5%)

Table 4.18: Immunolocalization of HHV-6 p41/38 and gp116/64/54 in paraffin-embedded cervical tissue

Histological Type	Total positive	Cytoplasm	Nucleus	Cytoplasm and Nucleus
Keratinizing squamous cell carcinoma	4	1	2	1
Nonkeratinizing squamous cell carcinoma	4	0	2	2
Adenocarcinoma	3	0	2	1
Carcinoma *in situ*	3	0	3	0
Normal	5	4	0	1

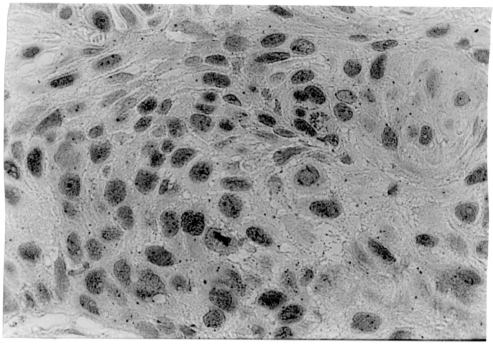

Figure 4.24: IHC for HHV-6 p41/38 (reddish brown) in the nuclei and cytoplasm of an invasive keratinizing SCC of the cervix (400×).

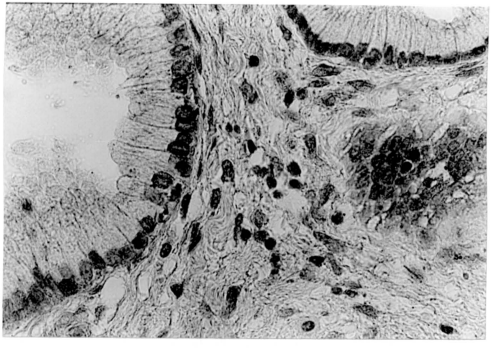

Figure 4.25: Immunohistochemical staining (p41/38) observed in the nuclei of endocervical columnar epithelial cells of a normal cervical biopsy (400×).

4.5 ANALYSES OF OTHER PARAFFIN-EMBEDDED TISSUE BIOPSIES

4.5.1 Formalin-fixed paraffin-embedded breast carcinoma tissue

Ten cases of carcinoma of the breast were included in the study to investigate the presence of HHV-6 infection. Tissue biopsies of 10 women, 7 Chinese and 3 Indians, whose ages ranged between 40 to 60 years with invasive breast carcinoma were studied. The histological status of these tissues are summarized in Table 4.19.

All 10 cases were subjected to nested PCR amplification of HHV-6 DNA and hybridized to labelled pZVH14 probe. No virus sequences were amplified in the samples. Since the DNA of all the cases were positive for β-globin sequence amplification, they were accepted as true negatives.

The presence of HHV-6 DNA sequences *in situ* were determined by NISH of tissue sections (Fig. 4.26). Immunohistochemical studies were also performed (Fig. 4.27). Both these methods failed to detect HHV-6 DNA sequences or antigens (Table 4.20). Since these experiments were performed in the presence of appropriate controls, the samples were accepted as true negatives and occasionally used as negative controls in NISH and IHC.

Table 4.19: Histopathology of paraffin-embedded tissue biopsies of breast carcinoma

Histological Type	No. of cases
Infiltrating ductal carcinoma	5
Infiltrating lobular carcinoma	2
Medullary carcinoma	2
Mucinous carcinoma	1
Total	10

Table 4.20 Human herpesvirus-6 positivity in paraffin-embedded breast carcinoma tissue

Histology	Nested PCR	Southern hybridization	NISH	IHC
Breast carcinoma	0	0	0	0

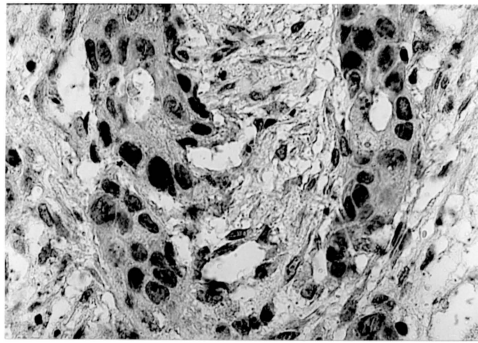

Figure 4.26: NISH negative staining for HHV-6 DNA in an infiltrating ductal carcinoma of the breast. The nucleus has been counterstained blue with Mayer's hematoxylin (400×).

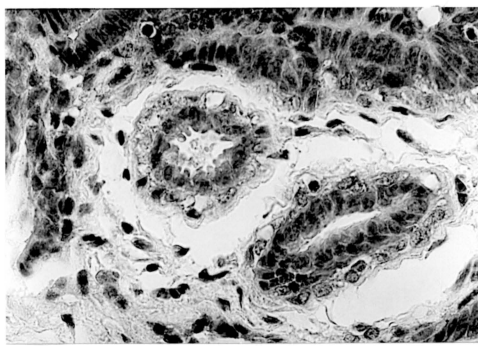

Figure 4.27: IHC negative staining for p41/38 in an infiltrating lobular carcinoma of the breast, the nucleus is counterstained blue (400×).

correlated with the results of NISH revealing the presence of HHV-6 proteins in all cases (Table 4.23). However, only 3/5 (60.0%) NPC cases expressed HHV-6 proteins in which the presence of HHV-6 DNA sequences correlated with the presence of HHV-6 protein expression.

Table 4.21: Detection of HHV-6 DNA sequences by PCR

Histology	Total samples	HHV-6 positive (%)	
		Nested PCR	Southern hybridization
Squamous cell carcinoma of the larynx	4	0	1 (25.0)
Nasopharyngeal carcinoma	5	0	2 (40.0)

Table 4.22: Prevalence of HHV-6 DNA detected by nonradioactive *in situ* hybridization

Histology	Total samples	HHV-6 Variant (%)			Total positive
		A	B	A and B	
Squamous cell carcinoma of the larynx	4	0	3 (75.0)	1 (25.0)	4 (100%)
Nasopharyngeal carcinoma	5	0	2 (40.0)	2 (40.0)	4 (80%)

Table 4.23: Prevalence of HHV-6-encoded proteins

Histology	Total sample	Reactivity to virus-encoded antigens (%)			Total positive
		p41/38	gp116/64/54	p41/38 and gp116/64/54	
Squamous cell carcinoma of the larynx	4	0	1 (25.0)	3 (75.0)	4 (100%)
Nasopharyngeal carcinoma	5	1 (20.0)	0	2 (40.0)	3 (60.0%)

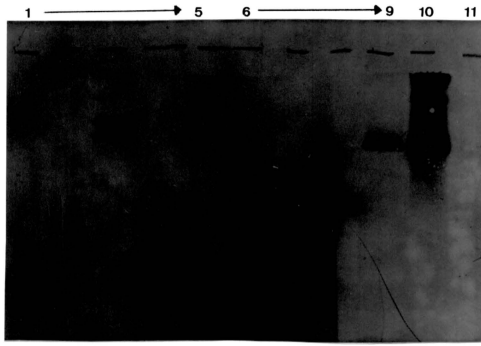

Figure 4.28: Southern blot hybridization of PCR amplified HHV-6 DNA sequences from paraffin-embedded lesions of the nasopharynx and larynx.

Lane 1-5 : DNA from nasopharyngeal carcinoma biopsies

Lane 6-9 : DNA from laryngeal SCC biopsies

Lane 10 : HHV-6 positive control

Lane 11 : HHV-6 negative control (water)

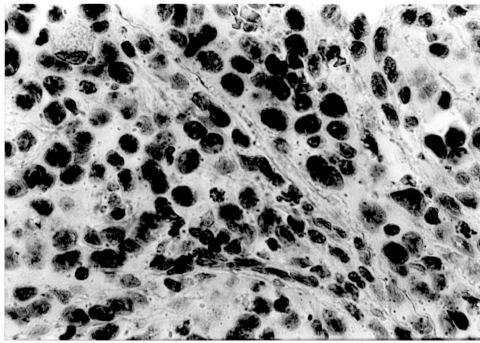

Figure 4.29: NISH signal (dark purple) for HHV-6B in the nuclei of a squamous cell carcinoma of the larynx (400×).

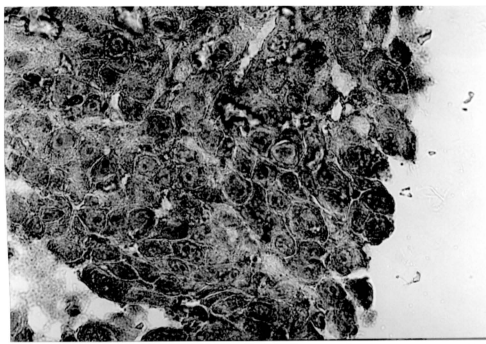

Figure 4.30: IHC positive staining for gp116/64/54 in the cytoplasm of a squamous cell carcinoma of the larynx (400×).

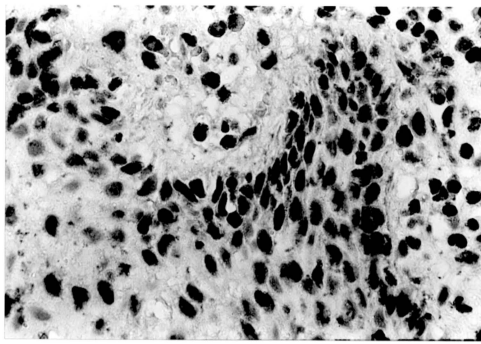

Figure 4.31: NISH signal (dark purple) for HHV-6B in the nuclei of a nasopharyngeal carcinoma (400×).